Journal of Advanced Research (2013) 4, 385–392

Cairo University

Journal of Advanced Research

ORIGINAL ARTICLE

# Synthesis and corrosion protection properties of poly(*o*-phenylenediamine) nanofibers

**P. Muthirulan, N. Kannan, M. Meenakshisundaram** *

*Centre for Research and Post-Graduate Studies in Chemistry, Ayya Nadar Janaki Ammal College (Autonomous), Sivakasi 626 124, Tamil Nadu, India*

Received 26 April 2012; revised 17 July 2012; accepted 17 July 2012
Available online 4 September 2012

**KEYWORDS**

Poly(*o*-phenylenediamine) nanofibers;
Oxidative polymerization;
316L SS;
Anticorrosive coatings;
3.5% NaCl

**Abstract** The present study shows a novel method for the synthesis of uniformly-shaped poly(othophenylediamine) (PoPD) nanofibers by chemical oxidative polymerization method for application towards smart corrosion resistance coatings. Transmission Electron Microscopy (TEM) and Scanning Electron Microscopy (SEM) studies confirm morphology of PoPD with three dimensional (3D) networked dendritic superstructures having average diameter of 50–70 nm and several hundred meters of length. UV–vis and FTIR spectral results shows the formation of PoPD nanofibers containing phenazine ring ladder-structure with benzenoid and quinoid imine units. Thermogravimetric analyses (TGA) of PoPD nanofibers possess good thermal stability. The anti-corrosion behavior of PoPD nanofibers on 316L SS was investigated in 3.5% NaCl solution using potentiodynamic polarization and electrochemical impedance spectroscopic (EIS) measurements. The PoPD coated 316L SS exhibits higher corrosion potential when compared to uncoated specimen. EIS studies, clearly ascertain that PoPD nanofiber coatings exhibits excellent potential barrier to protect the 316L SS against corrosion in 3.5% NaCl.



## Introduction

In recent years, intrinsically conducting polymers (ICPs) such as polyaniline, polypyrrole, polythiophene and their derivatives have been investigated for use in numerous potential applications, including rechargeable batteries, organic electronics, electrochromic devices and sensors [1]. One of the applications of conducting polymer is their use as surface coatings to protect metals against corrosion; it is an environment friendly and effective method. Several studies have been carried out recently or are in progress concerning the use of conducting polymer coatings for the corrosion protection of oxidizable metals [2,3].

Among the conducting polymers, poly(*o*-phenylenediamine) (PoPD), a highly aromatic polymer containing 2,3-diaminophenazine or quinoraline repeating unit has received significant attention because it can be utilized in many fields [4–6]. PoPD was first electrodeposited on 304 SS from aqueous solutions of phosphoric acid and sulfuric acid by D'Elia et al.

* Corresponding author. Tel.: +91 8940303090; fax: +91 4562254970.
E-mail address: chemistryanjac@gmail.com (M. Meenakshisundaram).

Peer review under responsibility of Cairo University.

ELSEVIER Production and hosting by Elsevier

2090-1232 © 2012 Cairo University. Production and hosting by Elsevier B.V. All rights reserved.
http://dx.doi.org/10.1016/j.jare.2012.07.007

[7] and by Hermas et al. [8] for corrosion protection application. The PoPD polymer has a ladder structure and different characteristics from those of PANI. Hermas [9] reported that PoPD passive film on steel, formed by electropolymerization, exhibits a superior resistance for pitting in aerated 3% NaCl compared with PANI film under similar experimental conditions.

In electropolymerization a careful choice of the solvent and/or the supporting electrolyte, and, the establishment of electrochemical parameters are necessary for the successful electrochemical synthesis of conducting polymer coatings on oxidizable metals. To overcome these difficulties, many efforts have been devoted to synthesize one-dimensional (1D) nano- or micro-structures of the material obtained from the chemical polymerization of conducting polymers [10–17]. Yao et al. [18] reported that the carbon steel coated with PANI nanofibers by chemical polymerization has excellent corrosion protection than that with aggregated PANI. Coatings prepared from polyaniline–nano-$TiO_2$ particles synthesized by in situ polymerization were found to exhibit excellent corrosion resistance compared to pure polyaniline (PANI) in aggressive environments [19]. Normally, micro- or nanofibers or nano-belts are obtained by solution polymerization through mixing [20], stirring [21], or reprecipitation [22], oligomers-assisting [23], seeding [24] or interfacial [25] processes. Recently, it has been reported that chloroauric acid shows good oxidative ability and can act as an oxidant for the oxidative polymerization of aniline [26], pyrrole [27], and *o*-phenylenediamine [28–30] to form their polymers. However, synthesis and the anti-corrosion properties of the PoPD nanofibers on 316L SS and other active metals have never been reported.

Concerning the formation mechanisms of conducting polymer (PANI and its derivative) nanofibers, it was stated that the newly formed primary PANI nanofibers, whose formation mechanism is still unclear, at the interface were continually withdrawn into the aqueous phase and separated with the monomers, leading to the continuing formation of the primary PANI nanofibers and the effective suppression of the secondary growth of the primary nanofibers. In the case of rapid mixing polymerization, aniline and the oxidant were consumed during formation of the primary nanofibers and the secondary growth of the primary nanofibers was suppressed then. Based on the results of these novel approaches and the fact new chemistry can be generated by using ultrasonic irradiation in preparing nano-materials due to its cavitation and vibration effect. However, synthesis by ultrasonication and the anti-corrosion properties of the PoPD nanofibers on 316L SS and other active metals have never been reported [31].

Stainless steel (SS) is being increasingly used as a structural material in marine and petrochemical applications. This is mainly due to its high corrosion resistance, high strength and toughness. However, in the presence of chloride ions, localized corrosion such as pitting and crevice corrosion is still a serious problem for such a materials [32–34]. Hence, the study on SS in chloride medium to enhance protection from corrosion has been of technological importance.

In this paper, (i) a novel synthesis protocol is presented for the preparation of PoPD nanofibers from *o*-phenylenediamine/$HAuCl_4$/PVP aqueous solution at room temperature by ultrasonic agitation, (ii) to confirm the structure and morphology of the PoPD nanofibers using UV–vis, FTIR, CV, TGA, TEM and SEM studies (iii) to investigate the corrosion inhibition performance of the PoPD film on 316L SS in 3.5% NaCl solution.

## Experimental

### *Chemicals*

Monomer *o*-phenylenediamine (oPD) and auric chloride ($HAuCl_4$) and polyvinylpyrrolidone (PVP) (Mw ~55,000) were purchased from Sigma–Aldrich. Polyvinyl butyral (PVB) (Mw 60,000) was obtained from SRL and used without further purification. Aqueous electrolytes used for the synthesis of the materials were prepared in double distilled water.

### *Synthesis and coatings of PoPD nanofiber on 316L SS*

The PoPD nanofibers were prepared by controllable chemical oxidative polymerization route. In the experimental procedure, 1 g of PVP and 1 g of oPD monomer were dissolved in 10 and 20 mL of double distilled water, respectively, under vigorous magnetic stirring to form homogeneous solutions at room temperature. Aliquots of the 2 mL of PVP and 12 mL of oPD were taken from these as-prepared solutions and mixed. The mixed solution was then diluted with 10 mL of double distilled water, and 0.2 mL of $HAuCl_4$ (10 mM) was added drop by drop. The solution quickly turned purple-red and became turbid in 5 s. The conical flask was then subjected to ultrasonication for 45 min at room temperature and the product was centrifuged and washed several times with double-distilled water. The polymerization mechanism is represented in scheme 1.

PVB (2 g) was dissolved in methanol (20 mL) and 10 wt.% of PoPD nanofibers powder was added and subjected to sonication for 45 min. This yielded a uniform dispersion of PoPD nanofiber in the PVB solution. The 316L SS samples of $10 \times 20 \times 2\ mm^3$ size were mechanically polished with 120–1000 grit silicon carbide papers followed by polishing with diamond paste to obtain mirror finish. The steel was then washed thoroughly with running distilled water, rinsed and ultrasonically degreased with acetone and then dried. This pretreated steel with a surface area of $0.5\ cm^2$ was then dip coated with the PoPD nanofiber/PVB in methanol solution and dried at 60 °C temperature for 45 min.

### *Instrumentation*

UV–vis spectra were recorded using "TECHCOMP" UV–vis spectrometer of model 8500 using a matched pair of Teflon Stoppard quartz cuvettes of path length 1 cm. FT-IR spectra were recorded using "BRUKER" (model TNSOR 27) in the region 4000–400 $cm^{-1}$ as KBr pellets. The TEM images were obtained with Hitachi model H-800 and SEM image was obtained using LEO 440 I model. Thermograms were recorded using a Perkin Elmer Thermal Analyzer over a temperature range of 100–1000 °C in an inert atmosphere at a heating rate of 10 °C $min^{-1}$.

A conventional three electrode cell was used for all the electrochemical measurements. A saturated calomel electrode (SCE) was used as reference electrode, platinum foil acts as a counter electrode and 316L SS as the working electrode. Potentiodynamic polarization and Electrochemical Impedance Spectroscopy measurements were carried out for the test

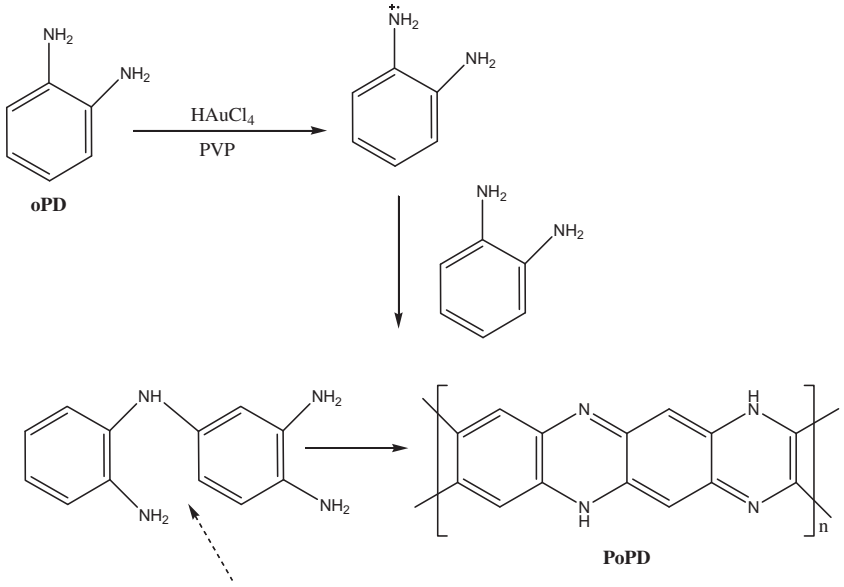


**Scheme 1** Schematic representation of polymerization mechanism of PoPD.

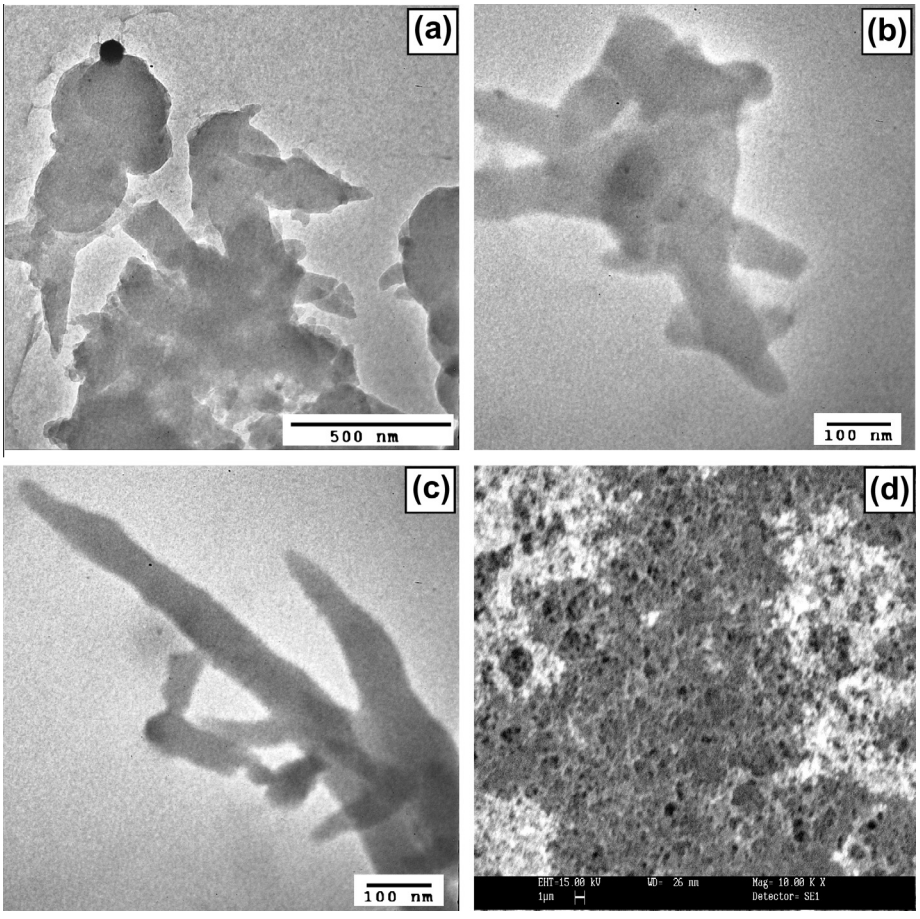


**Fig. 1** TEM (a–c) and SEM images (d) of PoPD nanofiber.

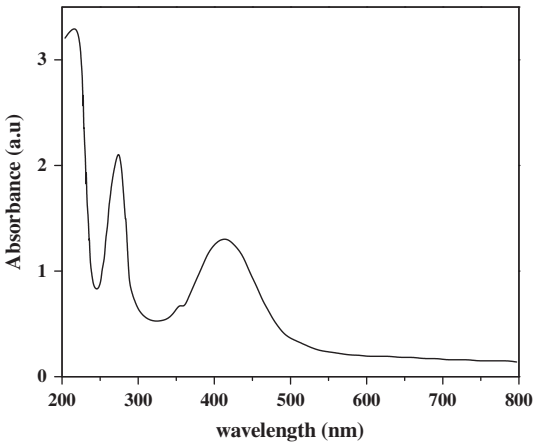


**Fig. 2** UV–vis spectra of PoPD nanofiber.

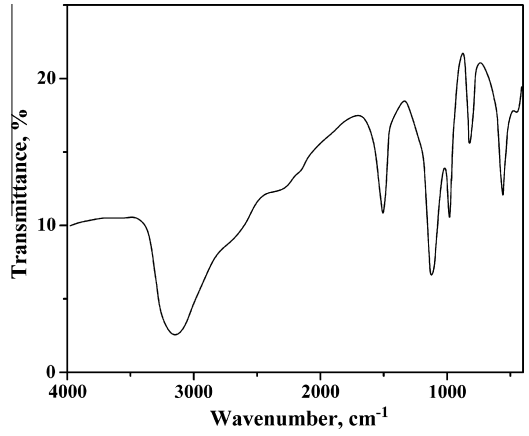


**Fig. 3** FT-IR spectra of PoPD nanofiber.

specimens in 3.5% NaCl solution using Potentiostat/Galvanostat (CH Instruments, model 1100A, USA).

## Results and discussion

### *TEM and SEM analysis of PoPD nanofibers*

The TEM images of the PoPD nanofibers that were synthesized by three different concentrations of PVP ((a) absence of PVP (b) 0.3 g of PVP and (c) 0.6 g of PVP) containing 0.1 g of monomer in 10 mL water are shown in Fig. 1. The absence of PVP results in the formation of PoPD polymer microspheres with an average diameter of 250–300 nm (Fig. 1a). Moreover, in the presence of PVP leads the formation of PoPD in nanofibers morphology with an average diameter of 50–70 nm width and several hundred nanometers of length (Fig. 1b and c). These results indicate that by increasing the PVP concentration there is a decrease in the diameter and an increase in the length of the PoPD nanofiber. This is due to the anisotropic growth of the conducting polymer [26–31]. This may be the result of the selective adsorption of PVP on certain surfaces, which hinders their growth. Thus, when the concentration of PVP is high, this kind of adsorption becomes stronger; hence the final particles become narrower in diameter and longer in length. The elongated form (fiber) is established as the growth rate for PoPD is distinctly not identical in all directions. Moreover the new active nucleation centers can be formed on initially formed nanofibers for the additional growth of nanofibers resulting in a branched network or dendrites (secondary nucleation). As it is obvious from the SEM image (Fig. 1d), the PoPD nanofibers are inter-connected to form dendritic and three-dimensional (3D) networked structures with highly branched geometry.

### *UV–vis and FTIR analysis*

The UV–vis spectra of oPD and PoPD were shown in Fig. 2. The peak located at 295 $cm^{-1}$ can be assigned to the $\pi$ to $\pi^*$ transition of the benzenoid rings, and the band at 428 $cm^{-1}$ suggests the existence of quinoid imine units (—C═N—) [26–29]. From the spectroscopic analysis, it can be concluded that the synthesized PoPD has a head-to-tail type arrangement with the benzenoid and quinoid structures in the phenazine-like backbone.

Fig. 3 shows the FTIR spectrum for PoPD film. PoPD is a ladder polymer, and the characteristic peaks at 3458, 1636, 1213, and 878 $cm^{-1}$ can be assigned to N—H stretching, quinoid stretching, C—N stretching, and the presence of the phenazine ring, respectively. The bands at 1057 and 588 $cm^{-1}$ are assigned to the oxalate dopant [26–29]. The UV–vis and FTIR spectroscopy results confirmed the formation of the PoPD film containing phenazine ring ladder-structure with benzenoid and quinoid imine units.

### *Cyclic voltammetry analysis*

Cyclic voltammetric response of uncoated and PoPD nanofiber coated 316L SS in 0.1 M NaCl solution at the scan rate of 50 mV $s^{-1}$ is depicted in Fig. 4. The oxidation ($E_{pa}$) and reduction ($E_{pc}$) peak potentials were −135 mV and −182 mV, respectively, showed no variation with cycling. The charge transfer reaction was quasi-reversible with the separation of peak potential ($\Delta E_p$ = 317 mV). This behavior is similar to that reported for PoPD films obtained by electrochemical deposition method on noble electrodes [5,23] and consequently the structure of the PoPD film grown on steel is expected to be similar. The proposed structure of the PoPD was represented as ladder polymer containing phenazine rings with an asymmetrical "quinoid" structure, and the expected redox reaction is as follows [35–37].

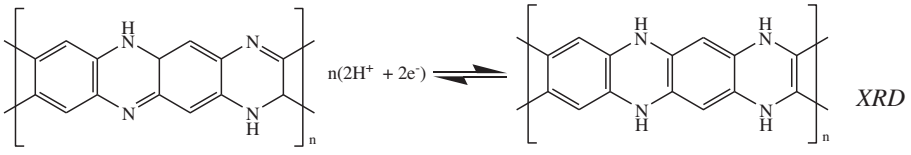

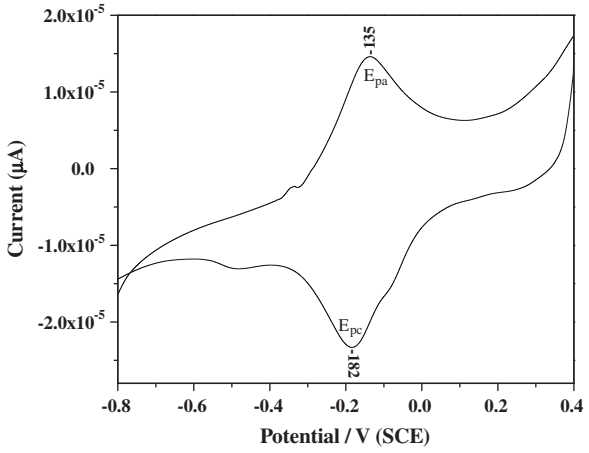


**Fig. 4** Cyclicvoltammogram of PoPD nanofiber coated 316L SS in 0.1 M NaCl at scan rate 50 mV $s^{-1}$.

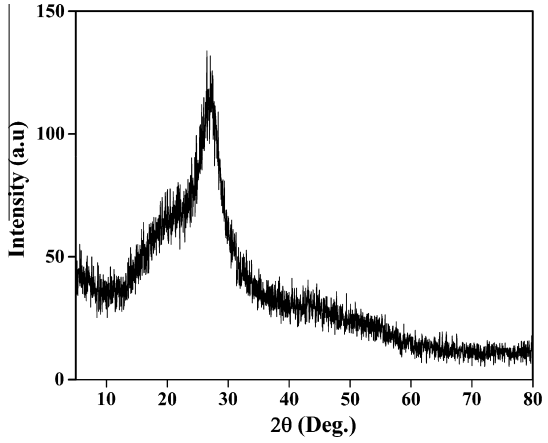


**Fig. 5** XRD spectra of PoPD nanofiber.

*XRD analysis*

The XRD spectrum (Fig. 5) of the PoPD film show the broad peak centered at $2\theta = 25°$ revealing that the local crystallinity may be caused by the periodicity perpendicular to the polymer chain. The partial crystallinity may be resulted from the long range ordering of polymer chains in PoPD back bone. Moreover, the diffraction peaks related to Au cannot be found in the XRD patterns, strongly indicating that the product is the pure poly(*o*-phenylenediamine) networks [36,37].

*Thermogravimetric analysis*

Thermogravimetric analysis (TGA) was used to examine the thermal stability of PoPD nanofiber and oPD monomer. PoPD nanofibers have a three stage thermal transition that lead to weight loss (Fig. 6). The first thermal transition observed at 150.6–240 °C was related to the removal of moisture. The second thermal transition occurred at 240–312 °C which corresponded to the loss of low molecular weight oligomers and side products. The third transition was observed between 312 °C and 700 °C with a weight loss of ~50%, which can attributed to the degradation of the backbone units of the PoPD (benzenoid and quinonoid units) [36]. Moreover PoPD nanofibers possess good thermal stability than the PANI and poly(phenylenediamine)s [36–40]. This may be due to the presence of ladder back bone in the PoPD structure.

*Surface morphological studies of uncoated and PoPD nanofibers in PVB coated 316L SS*

Fig. 7a and b shows the SEM micrographs of uncoated 316L SS and PoPD nanofiber coated 316L SS, respectively, with the same magnification. It is very clear from the figure that uncoated 316L SS surface exhibits smooth morphology. However, thin, uniform and closely packed continuous nodular

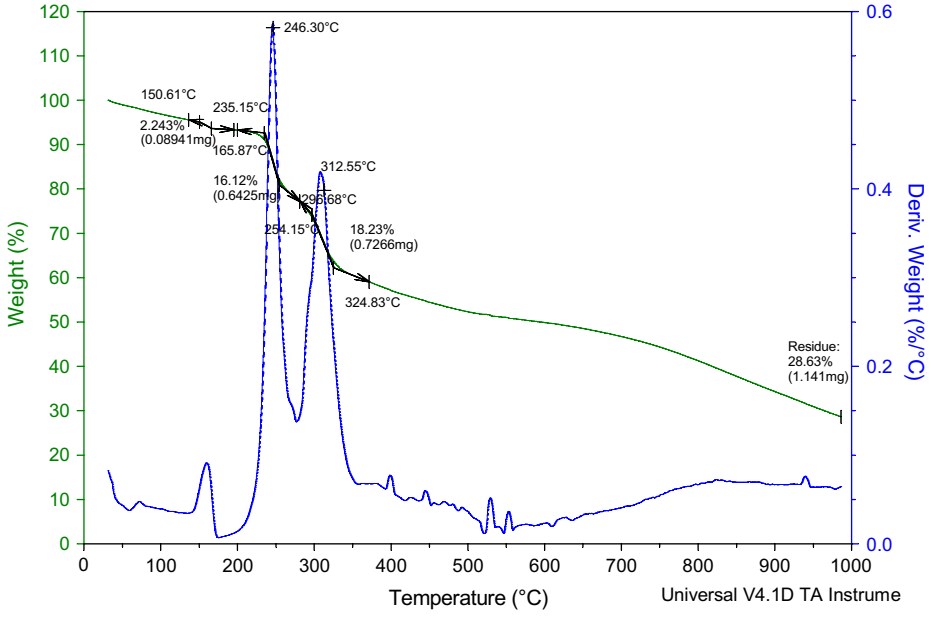


**Fig. 6** Thermogravimetric analysis of PoPD nanofiber.

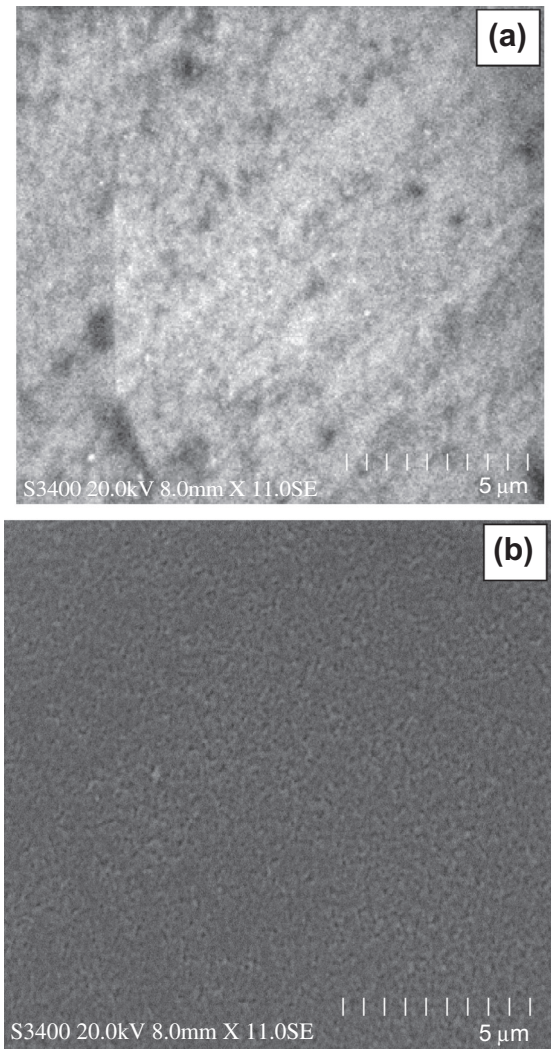


**Fig. 7** SEM images (a) uncoated and (b) PoPD nanofiber 316L SS.

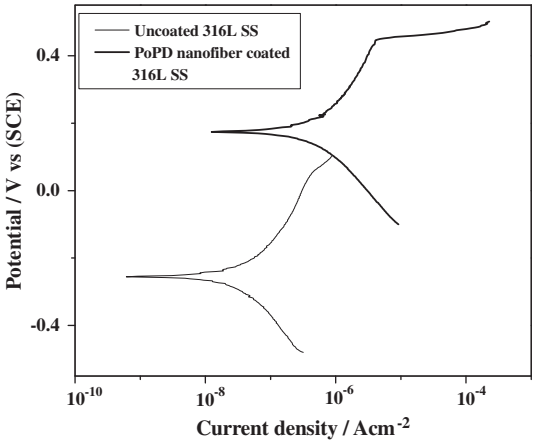


**Fig. 8** Potentiodynamic polarization studies of uncoated and PoPD nanofiber coated 316L SS in 3.5% NaCl solution.

film without any holes and scratches covering the entire 316L SS surface was observed for the PoPD nanofiber coated 316L SS.

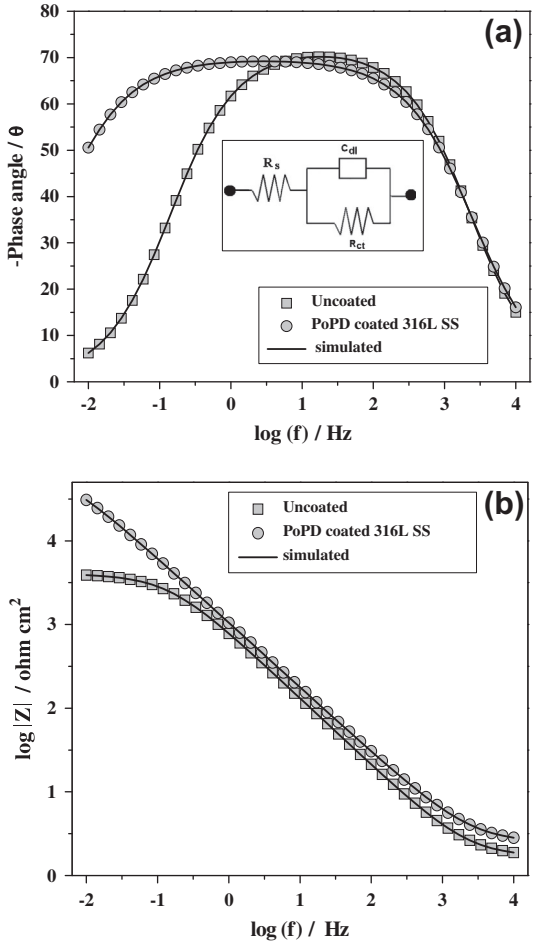


**Fig. 9** (a) Bode plots Phase angle and (b) Bode resistance plots for uncoated and PoPD nanofiber coated 316L SS in 3.5% NaCl solution.

*Electrochemical corrosion behavior of PoPD nanofiber coated 316L SS using potentiodynamic polarization and EIS measurements*

Fig. 8 shows the potentiodynamic polarization curves for uncoated and PoPD nanofiber coated 316L SS steel in 3.5% NaCl solution. It was observed that the PoPD nanofiber coated 316L SS exhibited higher corrosion potential ($E_{corr}$) and current density ($I_{corr}$) compared to uncoated 316L SS. The $E_{corr}$ shifts, from −256 mV to a more positive value of 174 mV when the steel surface was covered by the PoPD nanofiber film. The positive shift in $E_{corr}$ confirms the best protection of the SS when its surface is covered by the PoPD nanofiber. This indicates that PoPD nanofiber coating on 316L SS steel acts as a protective layer, which may be due to the presence of $\pi$ electrons in the aromatic ring and the lone pair of electrons in the nitrogen atom leads to the effective surface modification of 316L SS steel against corrosion. The thin, compact fibriform morphology covering the entire surface of 316L SS is thought desirable as an electrode material for inhibitors, because it can enable the effective and rapid passivation of SS, which results in high corrosion protection. It has been shown that conducting polymer coatings can either act as a physical barrier toward corrosive agents, or as inhibitory by

**Table 1** Electrochemical corrosion parameters for uncoated and PoPD nanofiber coated 316L SS in 3.5% NaCl solution.

| 316L SS | $E_{corr}$ (mV) | $I_{corr}$ (A cm$^{-2}$) | $\beta_a$ (mV dB$^{-1}$) | $\beta_c$ (mV dB$^{-1}$) | $R_p$ (Ω) | CR (mmpy) |
|---|---|---|---|---|---|---|
| Uncoated | −256 | $1.821 \times 10^{-8}$ | 41 | 39 | $1.37 \times 10^{5}$ | $2.20 \times 10^{0}$ |
| PoPD coated | 174 | $1.146 \times 10^{-7}$ | 19 | 16 | $3.97 \times 10^{5}$ | $1.38 \times 10^{-3}$ |

**Table 2** Electrochemical Impedance parameters of uncoated and PoPD nanofiber coated 316L SS in 3.5% NaCl solution.

| 316L SS | $R_s$ (Ω cm$^2$) | $R_{ct}$ (Ω cm$^2$) | $C_{dl}$ (μF cm$^{-2}$) | $n$ | Inhibition efficiency (%) |
|---|---|---|---|---|---|
| Uncoated | 1.67 | 4.05 | 270 | 0.80 | – |
| PoPD coated | 3.09 | 60.30 | 229 | 0.83 | 93 |

shifting the corrosion potential of the substrate to higher values thereby reducing the corrosion rate [2,36,37].

The electrochemical corrosion parameters were obtained from the extrapolation of Tafel and are given in Table 1. The corrosion rate of PoPD nanofiber coated steel was found to be ~0.004 mmpy$^{-1}$ which is ~1500 times lower than that observed for bare 316L SS. From the table, the nanofiber coated SS shows increased corrosion current density ($1.146 \times 10^{-7}$ A cm$^{-2}$) when compared to the uncoated SS ($1.821 \times 10^{-8}$ A cm$^{-2}$). The increase of the corrosion current density could be due to the doped, conductive character of the PoPD film, i.e., oxidation of the film and insertion of chloride anions as counter ions in the polymer structure [36,37,41].

EIS is widely used to characterize the corrosion protection performance of coating systems. Bode phase angle and resistance plots are illustrated in Fig. 9. From the Bode phase angle plots (Fig. 9a), the uncoated 316L SS showed less capacitive behavior in the middle frequency region, and, the phase angle value decreased in the low frequency region. This linear portion observed in the low frequency region indicates the dissolution of the metal ions in the solution. However, PoPD nanofiber film coated specimen showed increase in the maximal phase angle value, which indicates the enhancement of the resistive behavior of the protective layer due to the coating on the surface of 316L SS steel. The obtained impedance spectra was fitted using an equivalent circuit (Fig. 9a-inset) consisting of a capacitance with interfacial double layer ($C_{dl}$) in parallel with charge transfer resistance ($R_p$), both in series with solution resistance. $R_p$ and $C_{dl}$ jointly represent the electrochemistry of corrosion at the polymer–metal interface after coating penetration by corrosive ions [36,37,41].

The percent inhibition efficiency (IE%) of MS coated with polymer was calculated as follows [4].

$$\mathrm{IE}\% = \frac{R_{ct}(\text{coated}) - R_{ct}(\text{uncoated})}{R_{ct}(\text{coated})} \quad (1)$$

where $R_{ct}$(coated) and $R_{ct}$(uncoated) are the charge transfer resistance values with and without polymer coatings respectively. It was also shown that the coated specimen exhibited higher impedance values compared to uncoated specimen. The percentage of corrosion inhibition efficiency for the PoPD coated MS is 93%

Table 2 shows the fitted impedance data for uncoated and PoPD coated 316L SS. The lower resistance value for the uncoated 316L SS indicates the susceptibility of the substrate surface of being attacked by the ions present in the electrolyte, attributed to the thinning process of the passive film in 3.5% NaCl. However, higher $R_p$ values and lower $C_{dl}$ values for PoPD nanofiber coated 316L SS can be related to the increased degree of corrosion protection in 3.5% NaCl solution.

The Bode resistance plot for uncoated and PoPD nanofiber coated 316L SS in 3.5% NaCl solution are given in Fig. 9b. It can be observed that PoPD coated 316L SS exhibits higher corrosion resistance compared to uncoated 316L SS. This shows the corrosion protection of PoPD coated 316L SS in 3.5% NaCl medium.

## Conclusions

PoPD nanofiber was synthesized by polymerization of *o*-phenylenediamine using PVP and $HAuCl_4$ under ambient conditions. The structure and morphology of the PoPD nanofibers were characterized by UV, FTIR, SEM and TEM. Thin, adherent and compact layer of PoPD nanofibers were coated on 316L SS by dip coating method. The evaluation of corrosion behaviors for PoPD nanofiber coated 316L SS in 3.5% NaCl revealed that the corrosion potential shifted in the nobler direction which indicates the strong adherent and inhibition effect of the PoPD nanofiber film. The EIS show that the passive film of PoPD nanofiber coated on 316L SS exhibits good corrosion resistance when compared uncoated 316L SS. Hence, PoPD nanofiber coatings can be considered as a potential coating material for 316L SS in chloride containing medium.

## References

[1] Medany SS, Ismail KM, Badawy WA. Kinetics of the electropolymerization of aminoanthraquinone from aqueous solutions and analytical applications of the polymer film. J Adv Res 2012;3(3):261–8.
[2] Kilmartin PA, Trier L, Wright GA. Corrosion inhibition of polyaniline and poly(o-methoxyaniline) on stainless steels. Synth Met 2002;131:99–109.
[3] De Berry DW. Modification of the electrochemical and corrosion behavior of stainless steels with electroactive coatings. J Electrochem Soc 1985;132:1022–6.
[4] Muthirulan P, Rajendran N. Development of conducting polymer-Al2O3 hybrid nanocomposites for corrosion protection of mild steel. In: AIST steel properties and applications conference proceedings – materials science and, technology; 2010. p. 745–55.
[5] Sivakkumar SR, Saraswathi R. Application of poly(o-phenylenediamine) in rechargeable cells. J Appl Electrochem 2004;34:1147–52.
[6] Losito L, Palmisano F, Zambonin P. *O*-phenylenediamine electropolymerization by cyclic voltammetry combined with electrospray ionization-ion trap mass spectrometry. Anal Chem 2003;75:4988–95.

[7] D'Elia LF, Ortiz RL, Marquez OP, Marquez J, Martinez Y. Electrochemical deposition of poly(*o*-phenylenediamine) films on type 304 stainless steel. J Electrochem Soc 2001;148:C297–300.
[8] Hermas AA, Wu ZX, Nakayama M, Ogura K. Passivation of stainless steel by coating with poly(*o*-phenylenediamine) conductive polymer. J Electrochem Soc 2006;153:B199–205.
[9] Hermas A. Protection of type 430 stainless steel against pitting corrosion by ladder conductive polymer. Prog Org Coat 2008;61:95–102.
[10] Sun X, Dong S, Wang E. Formation of o-phenylenediamine oligomers and their self-assembly into one-dimensional structures in aqueous medium. Macromol Rapid Commun 2005;26:1504–8.
[11] Tian J, Liu S, Sun X. Supramolecular microfibrils of o-phenylenediamine dimers: oxidation-induced morphology change and the spontaneous formation of Ag nanoparticle decorated nanofibers. Langmuir 2010;26:15112–6.
[12] Sun X, Dong S, Wang E. Large-scale synthesis of micrometer-scale single-crystalline au plates of nanometer thickness by a wet-chemical route. Angew Chem Int Ed 2004;43:6360–3.
[13] Liu S, Wang L, Luo Y, Tian J, Lia H, Sun X. Polyaniline nanofibres for fluorescent nucleic acid detection. Nanoscale 2011;3:967–9.
[14] Sahay R, Suresh Kumar P, Sridhar R, Sundaramurthy J, Venugopal J, Mhaisalkar SG, et al. Electrospun composite nanofibers and their multifaceted applications. J Mater Chem 2012;22:12953–71.
[15] Tran HD, Kaner RB. A general synthetic route to nanofibers of polyaniline derivatives. Chem Commun 2006:3915–7.
[16] Huang J, Kaner RB. The intrinsic nanofibrillar morphology of polyaniline. Chem Commun 2006:367–76.
[17] Li D, Kaner RB. Processable stabilizer-free polyaniline nanofiber aqueous colloids. Chem Commun 2005:3286–8.
[18] Yao B, Wang G, Ye J, Li X. Corrosion inhibition of carbon steel by polyaniline nano-fibers. Mater Lett 2008;62:1775.
[19] Radhakrishnana S, Sijua CR, Mahantab D, Patil S, Madras G. Conducting polyaniline-nano-$TiO_2$ composites for smart corrosion resistant coatings. Electrochim Acta 2009;54:1249–54.
[20] Sun X, Hagner M. Mixing aqueous ferric chloride and *o*-phenylenediamine solutions at room temperature: a fast, economical route to ultralong microfibrils of assemblied *o*-phenylenediamine dimers. Langmuir 2007;23:10441–4.
[21] Guo S, Dong S, Wang E. Gram-scale, low-cost, rapid fabrication of high-quality width-controlled one-dimensional conducting polymer nanobelts. Chem Mater 2007;19:4621–3.
[22] Jiang HQ, Sun XP, Huang MH, Wang YL, Li D, Dong SJ. Rapid self-assembly of oligo (*o*-phenylenediamine) into one-dimensional structures through a facile reprecipitation route. Langmuir 2006;22:3358–61.
[23] Li W, Wang H. Oligomer-assisted synthesis of chiral polyaniline nanofibers. J Am Chem Soc 2004;126:2278–9.
[24] Zhang XY, Goux WJ, Manohar SK. Synthesis of polyaniline nanofibers by nanofiber seeding''. J Am Chem Soc 2004;126:4502–3.
[25] Huang JX, Kaner RB. A general chemical route to polyaniline nanofibers. J Am Chem Soc 2004;126:851–5.
[26] Yong W, Liu ZM, Han BX, Sun ZY, Ying H, Yang GY. Facile synthesis of polyaniline nanofibers using chloroaurate acid as the oxidant. Langmuir 2005;21:833–6.
[27] Selvan ST, Spatz JP, Klok HA, Moller M. Gold-polypyrrole core-shell particles in di-block copolymer micelles. Adv Mater 1998;10:132–4.
[28] Sun XP, Dong SJ, Wang EK. Large scale, templateless, surfactantless route to rapid synthesis of uniform poly(o-phenylenediamine) nanobelts. Chem Commun 2004:1182–3.
[29] Wang JJ, Jiang J, Hu B, Yu SH. Uniformly shaped poly(*p*-phenylenediamine) microparticles: shape-controlled synthesis and their potential application for the removal of lead ions from water. Adv Funct Mater 2008;18:1105–11.
[30] Wang L, Guo S, Dong S. Facile synthesis of poly(*o*-phenylenediamine) microfibrils using cupric sulfate as the oxidant. Mater Lett 2008;62:3240–2.
[31] Jing X, Wang Y, Wu D, Qiang J. Sonochemical synthesis of polyaniline nanofibers. Ultrason Sonochem 2007;14:75–80.
[32] Lo KH, Shek CH, Lai JKL. Recent developments in stainless steels. Mater Sci Eng R 2009;65:39–104.
[33] Bereket Gozen, Hur Evrim, Sahin Yucel. Electrodeposition of polyaniline, poly(2-iodoaniline), and poly(aniline-co-2-iodoaniline) on steel surfaces and corrosion protection of steel. Appl Surf Sci 2005;252:1233–44.
[34] Lucio Garcıa MA, Smit MA. Study of electrodeposited polypyrrole coatings for the corrosion protection of stainless steel bipolar plates for the PEM fuel cell. J Power Sources 2006;158:397–402.
[35] Pournaghi-Azar MH, Habibi B. Electrocatalytic oxidation of methanol on poly(phenylenediamines) film palladized aluminum electrodes, modified by Pt micro-particles: comparison of permselectivity of the films for methanol. J. Electroanal Chem 2007;601:53–62.
[36] Muthirulan P, Rajendran N. Poly(o-phenylenediamine) coatings on mild steel: electrosynthesis, characterization and its corrosion protection ability in acid medium. Surf Coat Technol 2012;206:2072–6.
[37] Muthirulan P, Rajendran N. In-situ template synthesis of PoPD-$TiO_2$ nanocomposites for active anti-corrosive coatings on 316L SS. Int J Nanosci 2011;10:1–6.
[38] Ayad MM, Rehab AF, El-Hallag IS, Amer WA. Preparation and characterization of polyaniline films in the presence of N-phenyl-1,4-phenylenediamine. Euro Polym J 2007;43:2540.
[39] Zhang L, Chai L, Liu J, Wang H, Yu W, Sang P. PH manipulation: a facile method for lowering oxidation state and keeping good yield of poly(*m*-phenylenediamine) and its powerful Ag+ adsorption Ability. Langmuir 2011;27:13729–38.
[40] Li XG, Huang MR, RF Chen, Jin Y, Yang YL. Preparation and Characterization of poly(p-phenylenediamine-co-xylidine). J Appl Polym Sci 2001;81:3107–16.
[41] Yagan A, Pekmez NO, Yıldız A. Poly(N-ethylaniline) coatings on 304 stainless steel for corrosion protection in aqueous HCl and NaCl solutions. Electrochim Acta 2008;53:2474–82.